Electronic Supplementary Information

Materials and methods

Preparation of PDMS slabs: Negative-relief masters of the PDMS slabs are fabricated on polished silicon wafers in several steps. First, a 50/100 Å titanium/gold thin film is thermally evaporated onto the silicon wafer. This thin film provides the high contrast needed to align the reservoirs with the pore and the filters. Next, an 800 μm × 15 μm × 15 μm (L × W × H) line and two sets of five, 100 μm × 15 μm × 15 μm (L × W × H), lines of SU-8 2015 photoresist (Microchem) are lithographically patterned onto the substrate. These resist lines correspond to the pore and the filters, respectively, that are subsequently embedded into the PDMS. The pore cross-sectional area is chosen to be comparable to the size of the cells and the pore length to be 800 μm, thereby ensuring a sufficient signal-to-noise ratio in our measurements *(S1)*. After exposed areas of gold are removed using a standard gold etchant (Gold Etch-Type TFA, Transene Co.), negative reservoirs, 2000 μm × 600 μm × 30 μm (L × W × H), are lithographically patterned with SU-8 2015. PDMS (Sylgard 184) (10:1 pre-polymer : curing agent) is dispensed onto the master, degassed, and cured for at least 12 hours at 80 °C. Prior to measurement, PDMS slabs with the embedded pore and reservoirs are cut from each master. Access holes in each slab are created by coring the PDMS with a 16 G syringe needle. Each slab is then thoroughly cleaned with 18 MΩ deionized (DI) water and treated with an oxygen plasma (100 mT, 5 mA, 10 s) to 1) create a hydrophilic surface; and 2) bond permanently (after subsequent heating) the slab to the prepared glass substrate *(S2)*.

Preparation of electrodes: The electrodes are lithographically patterned onto glass substrates using AZ 3318D (Clariant) resist. A 50/250 Å Ti/Pt thin film is deposited using an electron-gun evaporator. Before sealing to the PDMS slab, the glass substrates are functionalized.

Device functionalization and assembly: The glass substrates with the pre-defined electrodes are first exposed to an oxygen plasma (100 mT, 5 mA, 10 s). The region between the electrodes is coated with amino-silane groups *(S3)* via micro-contact printing *(S4)* using a solution of 3-aminopropyltriethoxysilane (APTES) (Sigma Aldrich) in anhydrous toluene (10 % w/w) (Sigma Aldrich) at room temperature. To ensure a stable APTES layer, the substrate is baked in an oven at 80 °C for 4-5 hours, thereby cross-linking the APTES. Following baking, the cured substrate is soaked in toluene (10 min) and then soaked and rinsed in 18 MΩ DI water (twice, 10 min each) to remove any unbound APTES. Once the APTES is patterned, the glass substrate is oxygen-plasma treated (100 mT, 5 mA, 10 s), with the functionalized area protected with a clean PDMS slab. This PDMS slab is subsequently removed and the top of the substrate is coated with 2-4 μL of 18 MΩ DI water. This enables easy alignment of the PDMS slab embedded with the pore and reservoirs to the prepared substrate. Once aligned, the PDMS/glass substrate assembly is placed on a hot plate and subjected to a 10-min bake ramped from 65 °C to 150 °C. This bake drives off the water and induces a permanent bond between the PDMS and glass substrate. After sealing, a 5 mM solution of N-5-Azido-2-

nitrobenzoyloxysuccinimide (ANB-NOS) (Pierce Biotechnology), dissolved in dimethylsulphoxide (DMSO) (Sigma Aldrich) (10 % of the final reaction volume) in 20 mM HEPES (Invitrogen) (pH 7.3), is injected inside the pore. After an overnight incubation in the dark, the excess ANB-NOS is removed by washing the pore with HEPES (20 mM). A solution of protein is then injected into the pore and allowed to incubate for 3-4 hours. For the covalent binding of proteins with the ANB-NOS treated glass substrate, the device is placed directly under a UV-light source (Ushio 350DS, 365-405 nm, 350 W, 3 min) at a distance of 5 cm, thus activating the aryl-azide photoreactive groups. Excess protein is then flushed thoroughly through the device with buffer solution (1 × PBS at 25 °C).

Fluid handling: Pressure-driven flow across the reservoirs and pore is accomplished using a commercial microfluidic pump (Fluidigm). The pump is connected to the device through Tygon Microbore tubing (Fisher Scientific, 0.06-inch o.d. and 0.02-inch i.d.) that is inserted into the access holes of the PDMS slab.

Data acquisition and analysis: A four-point measurement of the current is performed using a constant applied DC voltage (typically 0.2–0.4 V), as described in Ref. *(S5)*. The current is passed through a preamplifier (DL Instrument 1211) that performs a low-pass filter at 0.3 ms in rise time. The resulting output is connected to a data acquisition board (National Instruments PCI-6035E) for data sampling at 50 kHz.

Data are recorded and analyzed using custom-written software. Pulses generated when two cells flow simultaneously across the pore have a characteristic shape (Supplementary Fig. S1) that are easily recognized and discarded.

Pulse shape and cell size analysis: For an aspherical particle with an axis of symmetry, the orientation of its axis of revolution with respect to the applied electric field affects the electrical resistance. If we assume $\left|\frac{\delta R}{R}\right| \approx \left|\frac{\delta I}{I}\right|$, the relationship between the normalized current ($\delta I/I$) and the volume ratio ($V_{\text{particle}}/V_{\text{pore}}$) is,

$$\frac{\delta I}{I} = \left[f_{\perp} + \left(f_{\parallel} - f_{\perp} \right) \cos^2 \alpha \right] \frac{V_{particle}}{V_{pore}} \qquad \text{(S1)}$$

where α is the angle between the electric field $\vec{E}$ and the axis of revolution. In Eq. (S1), $f_{\perp}$ and $f_{\parallel}$ are the shape factor's perpendicular and parallel components, respectively. $f_{\perp}$ and $f_{\parallel}$ are a function of the particle shape, which is defined by γ, the ratio between the particle's axis of revolution (a) to its equatorial axis (b) (Supplementary Fig. S2). Because $f_{\perp}$ and $f_{\parallel}$ are different for an aspherical particle, the resistive pulses show oscillations *(S6, S7)*. γ is directly related to the pore's diameter D and length L and the axial flow velocity v_o by,

$$\left(\frac{1+\gamma^2}{\gamma}\right) = T\left(\frac{2v_0}{\pi D}\right)\left(1-\frac{L}{\tau v_0}\right)^{1/2} \qquad \text{(S2)}$$

Here, T is the period of rotation of an aspherical particle tumbling through a blank pore (See text). For our measurements, we determined that MEL cells are oblate spheroids with γ=0.39 ± 0.12. This is consistent with the fact that these cells are precursors to erythrocytes. We optically confirmed γ using wide-field deconvolution microscopy (See below). Supplementary Fig. S3 shows a reconstructed three-dimensional image of an immobilized stained MEL cell: the cell is oblate with $\gamma \sim 0.35$. With γ measured, we were able to determine $f_{\perp}$ and $f_{\parallel}$ as described in Ref. *S6* and *S7*, and in turn, the size of the MEL cells.

We measured the MEL cell size from the analysis of pulse magnitudes in a blank pore. After Refs. *(S6)* and *(S7)*, only those pulses that clearly showed oscillations (~75 % of cells passing through the pore) were taken into account in the cell size analysis (Fig. 2b main text). The distribution of $\delta I/I$ obtained with a functionalized pore is slightly different than that obtained with a blank pore. This difference is most likely due to protein-protein interactions in the functionalized pore, which subsequently affects cell orientation and shape inside the pore. Thus, a blank pore should be used for a more accurate cell-size determination.

MEL cell staining: To determine optically the shape of an MEL cell, 10 µL of suspended cells (RPMI-1640) (Invitrogen) (~1.1×10^6 cells/mL) were placed into a 1.5 mL microcentrifuge tube with 10 µL of 3% (v/v) low-melt agarose (Apex) in 0.5 × TBE buffer (Invitrogen). The agarose was allowed to solidify by cooling the tube to slightly below 15 °C. The agarose block was incubated at 37 °C with 1 µL of cell-labeling solution (Vybrant DiI) (Invitrogen). After 24 hrs, the agarose block was then rinsed with RPMI-1640 (Invitrogen) at 37 °C and placed on a glass slide. Tape (120 µm-thick) was applied to both sides of the slide to provide a spacer between the slide and the coverslip that was eventually placed on top. After re-melting the agarose on a hot plate at 70 °C and adding ~10 µL of Vectashield Mounting Medium (H-1000) (Vector), a coverslip was placed on top of the slide and sealed with fingernail polish *(S8)*.

Wide-field deconvolution microscopy: Wide-field deconvolution microscopy was performed using an inverted fluorescent microscope (Olympus IX70) equipped with a movable z-axis stage that permitted imaging of the cell at different focus positions. Cell images were acquired using a 60× water objective (1.3 NA). The recorded images were deconvoluted using Huygens Essential software (Scientific Volume Imaging) and then analyzed with Imaris software (Bitplane).

Transit-time distribution analysis: We modeled the τ-distribution from a single population with a log-normal distribution. As an example, the fitted distributions corresponding to MEL and U937 cells flowing through a blank pore are shown in Figs. 2c and d (main text) and Supplementary Fig. S4, with the fitting parameters listed in

Supplementary Tables S1 and S2. To validate the goodness of our fitting, we utilized the Kolmogorov-Smirnov (K-S) test. Unlike the Chi-square goodness of fit, the K-S test is an exact test and does not depend on the sample size of the data. We calculated the *p*-values of observed test statistics using simulations, since the critical region of the K-S test is no longer valid when the distribution parameters in the test are estimated from the data (*S9*). The obtained *p*-values are quite large (Supplementary Tables S1 and S2), indicating good fitting of the data. As shown in Supplementary Fig. S4, the MEL and U937 τ-distributions are shifted apart by ~1 ms. This shift is most likely due to different cell properties (i.e. size, density, and stiffness) *(S10)*, although further experiments are needed to confirm this. Despite the transit-time shift, the two τ–distributions still overlap greatly.

For a mixture of MEL and U937 cells traveling across an anti-CD34 antibody pore (only the MEL cells interact specifically with the functionalized anti-CD34 antibodies), we modeled the transit time with a mixture of two log-normal distributions, with each mixture distribution component corresponding to a cell subpopulation. Particularly, as described in the text, we built a unified constrained model for the mixed MEL and U937 cells in ratios of 1:1, 1:3, and 1:9. The estimates of the fittings are presented in Supplementary Table S3. The fittings are plotted in the right column of Fig. 3. We used a K-S test to evaluate the goodness of fit. The global *p*-value for the constrained model is ~0.84, which suggests that the fitting is statistically acceptable.

Colloid preparation. Prior to use, 9.95 ± 0.46 μm SuperAvidin-coated polystyrene colloids (Bangs Laboratories) were washed in 0.5 × PBS, 0.1% (v/v) Tween 20 three times (9000g for 5 minutes). The functionalization of the colloids was achieved with biotinylated anti-human annexinV antibodies (R&D Systems): a solution of 3.7×10^5 colloids/mL was incubated with 5 μg/mL antibodies at room temperature for 30 minutes. Based on the manufacturer's supplied information, 1.11×10^7 SuperAvidin molecules were present on the surface of each colloid. Therefore, the minimum saturating concentration for a solution containing 3.7×10^5 colloids/mL is ~1.0 μg/mL. An excess of antibodies was used to ensure full coverage of the colloid surface. After incubation, excess antibodies were removed by washing the colloids in the above wash buffer. Functionalized colloids were then injected into a pore functionalized with annexinV (R&D Systems) (50 μg/mL) (Supplementary Fig. S5).

Supplementary Figures

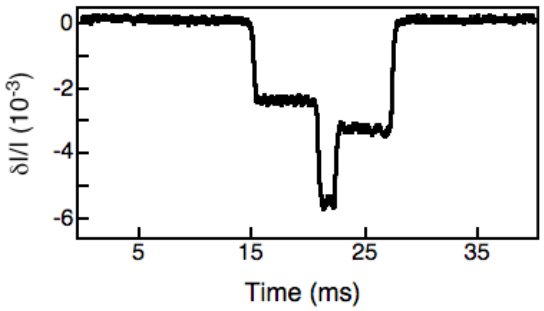

Supplementary Fig. S1. Pulse generated when two cells occupy the pore at the same time.

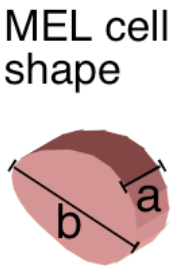

$$\gamma = a/b$$

Supplementary Fig. S2. Definition of γ as the ratio between the cell's axis of revolution (*a*) and its equatorial axis (*b*).

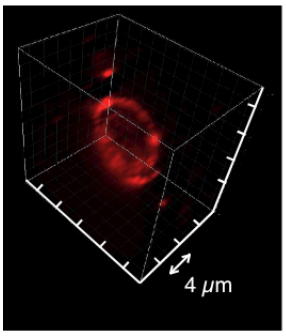

Supplementary Fig. S3. Reconstructed three-dimensional image of an MEL cell obtained with wide-field deconvolution microscopy.

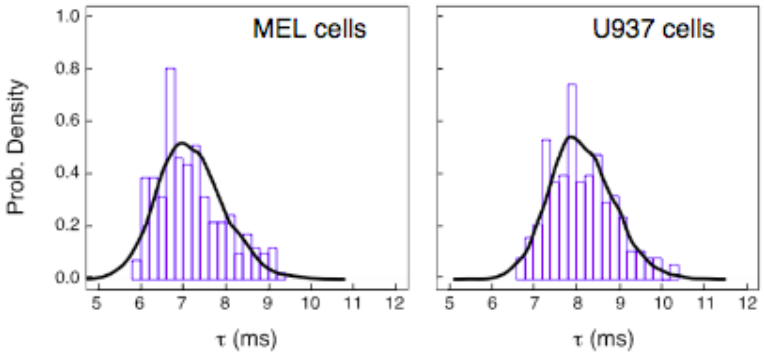

Supplementary Fig. S4. τ-distribution for a single population of MEL cells (left) and U937 cells (right) flowing (10.0 kPa) through a blank pore. Experimental data were fitted using a log-normal distribution (black line). The number of MEL and U937 cells measured was 206 cells and 189 cells, respectively.

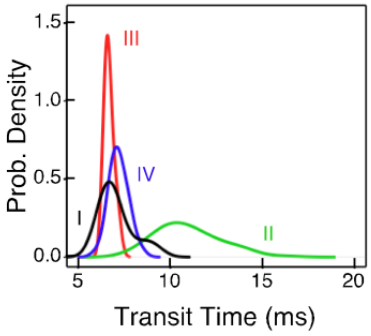

	I	II	III	IV
SuperAvidin Colloid	+	+	+	+
Annexin V Pore	-	+	-	+
Anti-annexin V Ab Colloid	+	+	-	-

Supplementary Fig. S5. Detection of anti-annexinV antibodies on the surface of uniformly-sized colloids. τ-distributions obtained when flowing uniformly-sized SuperAvidin polystyrene colloids (9.95 ± 0.46 μm). The + in each column (I-IV) indicates the presence of that component. Column I: colloids bound to anti-annexinV antibodies and flowed through a blank pore (data corresponds to the measurement of 120 colloids); Column II: colloids bound to anti-annexinV antibodies and passed through a pore functionalized with annexinV (data corresponds to 66 colloids); Column III: colloids passed through a blank pore (data corresponds to 53 colloids); and Column IV: colloids passed through a pore functionalized with annexinV (data corresponds to 61 colloids). τ_{avg} is greatest when the colloids are conjugated with anti-annexinV and pass through a pore functionalized with annexinV (Column II). τ_{avg} is 7.06 ms when the colloids are conjugated with anti-annexinV and pass through a blank pore and 10.95 ms when the same colloids pass through an annexinV pore.

Supplementary Tables

Experiment	μ	σ	*p*-value
MEL – Blank	1.815	0.037	0.955
MEL - IgG2a Ab. (100 μg/mL)	1.897	0.078	0.201
MEL - Anti-CD34 Ab. (100 μg/mL)	1.997	0.074	0.964
MEL - IgG2a Ab. (1500 μg/mL)	1.837	0.063	0.780
MEL - Anti-CD34 Ab. (1500 μg/mL)	2.349	0.096	0.572

Table S1. Log-normal fittings for MEL transit time (Figs. 2c and d, main text)

Cell Type	μ	σ	*p*-value
MEL	1.965	0.109	0.300
U937	2.090	0.092	0.643

Table S2. Log-normal fittings for the single cell populations (Supplementary Fig. S4)

Pore	MEL:U937	α_1	α_2	μ_1	σ_1	μ_2	σ_2
Anti-CD34 Ab.	1:1	0.532	0.468	2.444	0.144	2.198	0.084
Anti-CD34 Ab.	1:3	0.359	0.641	2.444	0.144	2.198	0.084
Anti-CD34 Ab.	1:9	0.089	0.911	2.444	0.144	2.198	0.084

Table S3. Log-normal model fittings for the mixed cell populations traveling in a pore functionalized with anti-CD34 antibodies (Fig. 3, main text)

Legend:

μ_i = mean of the distribution (*)

σ_i = standard deviation of the distribution (*)

p-value = statistical significance calculated with a Kolmogorov-Smirnov test

(*) Calculated after taking the logarithm of the data.

Supplementary References

S1. O. A. Saleh, and L. L. Sohn, *Rev. Sci. Instrum.*, 2001, **72**(12), 4449-4451.
S2. Y. N. Xia, and G. M. Whitesides, *Angew. Chem., Int. Ed.*, 1998, **37**, 551–575.
S3. S. Karrasch, M. Dolder, F. Schabert, J. Ramsden, and A. Engel, *Biophys. J.*, 1993, **65**, 2437-2446.
S4. J. L. Wilbur, A. Kumar, H. A. Biebuyck, E. Kim, and G. M. Whitesides, *Nanotechnology*, 1996, **7**(4), 452-457.
S5. O. A. Saleh, and L. L. Sohn, *Proc. Natl. Acad. Sci. U S A*, 2003, **100**(3), 820-824.
S6. D. C. Golibersuch, *J. Appl. Phys.*, 1973, **44**(6), 2580-2584.
S7. D. C. Golibersuch, *Biophys. J.*, 1973, **13,** 265-280.
S8. A. Chan and W. Z. Cande, *J. Cell Sci.*, 1998, **111**, 3507-3515.
S9. M. A. Stephens, *J. Am. Stat. Assoc.*, 1974, **69**, 730-737.
S10. M. J. Rosenbluth, W. A. Lam, and D. A. Fletcher, *Lab Chip*, web published June 5, 2008, and references therein.